

## The effect of chemical residues on the physical and electrical properties of chemical vapor deposited graphene transferred to SiO<sub>2</sub>

A. Pirkle,<sup>1</sup> J. Chan,<sup>1</sup> A. Venugopal,<sup>2</sup> D. Hinojos,<sup>1</sup> C. W. Magnuson,<sup>3</sup> S. McDonnell,<sup>1</sup> L. Colombo,<sup>4</sup> E. M. Vogel,<sup>1,2</sup> R. S. Ruoff,<sup>3</sup> and R. M. Wallace<sup>1,a)</sup>

<sup>1</sup>Department of Materials Science and Engineering, The University of Texas at Dallas, Richardson, Texas 75080, USA

<sup>2</sup>Department of Electrical Engineering, The University of Texas at Dallas, Richardson, Texas 75080, USA

<sup>3</sup>Department of Mechanical Engineering and Materials Science and Engineering Program, The University of Texas at Austin, One University Station C2200, Austin, Texas 78712, USA

<sup>4</sup>Texas Instruments Incorporated, Dallas, Texas 75265, USA

(Received 30 June 2011; accepted 4 September 2011; published online 23 September 2011)

The effects of residues introduced during the transfer of chemical vapor deposited graphene from a Cu substrate to an insulating (SiO<sub>2</sub>) substrate on the physical and electrical of the transferred graphene are studied. X-ray photoelectron spectroscopy and atomic force microscopy show that this residue can be substantially reduced by annealing in vacuum. The impact of the removal of poly(methyl methacrylate) residue on the electrical properties of graphene field effect devices is demonstrated, including a nearly 2 × increase in average mobility from 1400 to 2700 cm<sup>2</sup>/Vs. The electrical results are compared with graphene doping measurements by Raman spectroscopy. © 2011 American Institute of Physics. [doi:10.1063/1.3643444]

Growth of graphene on Cu substrates using chemical vapor deposition (CVD) is a promising approach for production of large-area graphene for device applications.<sup>1</sup> Previous experimental reports have demonstrated that continuous coverage of a uniform single layer of graphene can be readily achieved and that field effect transistors (FETs) with carrier mobility ranging from 10<sup>3</sup> to 10<sup>4</sup> cm<sup>2</sup>/Vs have been reported.<sup>2–4</sup> In order to fabricate electrically isolated devices, graphene must be transferred from Cu to an insulating substrate, such as SiO<sub>2</sub>. Device fabrication including lithographic patterning of graphene is carried out after the films are transferred to the dielectric.

Reports of transferred CVD graphene devices to date indicate that extrinsic scattering dominates the device properties, resulting in room temperature field effect mobility ranging between 200 and 2500 cm<sup>2</sup>/Vs, and significant resistance-voltage hysteresis is also observed.<sup>5–7</sup> It is well known that graphene is sensitive to scattering from charged impurities.<sup>8</sup> Several mechanisms for transient charging resulting in DC hysteresis have been considered in recent work employing pulsed I-V measurements, with species such as H<sub>2</sub>O trapped at the graphene/SiO<sub>2</sub> interface being a likely cause.<sup>7,9</sup> In the case of transferred CVD graphene, impurities and defects can be introduced during the transfer process. A common method for graphene transfer uses a polymer “handle” layer which comprises of spin-coated poly(methyl methacrylate) (PMMA) to support the graphene while the thin Cu substrate is etched away.<sup>10</sup> Removal of PMMA from graphene is problematic. Conventional semiconductor surface cleaning techniques cannot be employed as they inevitably damage or destroy the graphene layer. As a result, a common method employed for cleaning of graphene surfaces is annealing in a clean or reducing environment such as vacuum, H<sub>2</sub>/N<sub>2</sub> or H<sub>2</sub>/Ar.<sup>5,11,12</sup> Annealing in 1 atm of Ar at 200–400 °C has been shown to lead to an increase in p-type

doping in exfoliated graphene samples as measured by Raman spectroscopy; similar Raman results are presented in this work, but a *decrease* in p-type doping is observed for electrical measurements in vacuum.<sup>13</sup> In this Letter, the removal of PMMA from graphene by a combination of solvent (acetone) followed by vacuum annealing is studied. This process is examined using x-ray photoelectron spectroscopy (XPS), atomic force microscopy (AFM), and Raman spectroscopy in conjunction with electrical characterization of back-gated graphene field effect devices under vacuum.

The CVD graphene samples employed in this work are grown on 25 μm thick Cu foils (Alfa Aesar, 99.8% purity) in a halogen lamp-based quartz tube furnace at a growth temperature of 1035 °C with 5 sccm of H<sub>2</sub> and 7 sccm of CH<sub>4</sub> flowing during growth with a total pressure of 400 Torr. Graphene grown by this method has a grain size of 10–20 μm as determined by scanning electron microscope imaging. The specific steps of the graphene transfer process are as follows.<sup>1</sup> First, PMMA (Aldrich, MW = 996 kDa) dissolved in chlorobenzene with a concentration of 46 mg/mL is spin-coated on graphene on Cu at a spin speed of 3000 rpm for 1 min followed by 1000 rpm for 1 min (acceleration of 1000 rpm/s). The resulting PMMA thickness is approximately 50 nm. The sample is then dried at 25 °C in laboratory ambient air for 12 h. The Cu substrate is etched in 3:1 DIW:HNO<sub>3</sub> for 1 min followed by etching in ammonium persulfate for approximately 3 h with the endpoint determined when Cu is no longer visible. The samples are then etched for an additional 15 h in a separate fresh ammonium persulfate bath to ensure that the Cu is completely removed. The resulting PMMA/graphene membrane is transferred to a rinse bath of isopropanol alcohol and is then drawn onto a SiO<sub>2</sub> substrate. The sample is then blown dry with N<sub>2</sub>, and baked in air on a hot plate at 220 °C for 5 min, allowing the PMMA to reflow as it is baked.<sup>10</sup> Once the sample has cooled, PMMA is stripped using acetone at 25 °C. Samples prepared using this method are referred to here as “transferred graphene.”

<sup>a)</sup>Author to whom correspondence should be addressed. Electronic mail: rmwallace@utdallas.edu.

XPS spectra were collected using a monochromatic Al K x-ray source and Omicron EA125 hemispherical analyzer. The spectrometer was configured with an acceptance angle of  $\pm 8^\circ$ , a takeoff angle of  $45^\circ$ , and a 15 eV analyzer pass energy. In order to correctly fit the C 1s XPS spectrum, the  $sp^2$  C-C peak corresponding to graphene is modeled using the asymmetric Doniach-Sunjc (DS) line shape.<sup>14</sup> The XPS C 1s spectrum of graphene on Cu prior to transfer (Fig. 1(a)) can be described by a single DS component with a full width at half maximum (FWHM) of 0.71 eV. The graphene  $sp^2$  components of the post-transfer C 1s spectrum shown in Figs. 1(b) and 1(c) are described by constraining the line shape to have a FWHM of 0.71 eV. In the post-transfer C 1s spectrum (Fig. 1(b)), spectral components corresponding to PMMA can be clearly identified by peak fitting. This indicates that PMMA is not completely removed from the graphene surface by acetone during the cleaning process described above. To overcome this problem, a 300 °C/3 h vacuum ( $1 \times 10^{-9}$  mbar) anneal was employed. XPS analysis (Fig. 1) shows a clear reduction in the intensity of the C 1s states associated with PMMA after annealing. The chemical states identified in Fig. 1 as (d) through (i) are attributed to functional groups of the PMMA molecule.<sup>15</sup> The post-anneal C 1s spectrum indicates that some PMMA is still present suggesting that further process improvement to completely remove this residue is possible.<sup>16</sup> AFM images of a  $5 \times 5 \mu\text{m}^2$  area of the transferred graphene sample before and after annealing are shown in Fig. 2. A rough surface is observed before annealing with a significant reduction in roughness and better uniformity after annealing.

Raman spectra were collected over a  $40 \times 40 \mu\text{m}^2$  area with  $1 \mu\text{m}$  step size in ambient air using a Nicolet Almega XR spectrometer with a 532 nm laser excitation source. The maps were analyzed by fitting a single Lorentzian peak to the G,

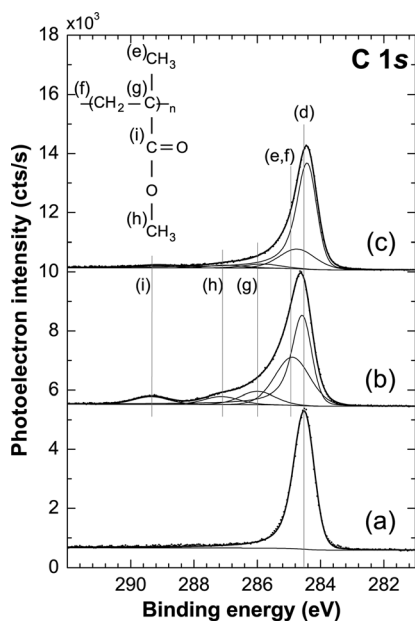


FIG. 1. XPS C 1s spectrum for (a) CVD graphene on Cu, (b) graphene after transfer to SiO<sub>2</sub> and removal of PMMA using acetone, and (c) after 300 °C/3 h UHV anneal. Curve fits to spectral components attributed to graphene  $sp^2$  C-C bonds (d) and PMMA residue (e)–(i) are shown.

2D, and D peaks of each spectrum after a linear background subtraction. After annealing, the mean position of the G (2D) peak is shifted by  $5.8 \text{ cm}^{-1}$  ( $2.8 \text{ cm}^{-1}$ ). Histogram plots of these peak-position distributions are shown in (Figs. 3(a) and 3(b)). The intensity ratio of the 2D and G peaks,  $I_{2D}/I_G$ , decreases from a mean value of 3.63 before anneal to 2.72 after anneal (Fig. 3(c)). The observed shifts in G and 2D peak positions as well as the decrease in  $I_{2D}/I_G$  ratios are consistent with an increase in p-type doping after vacuum.<sup>17,18</sup> The distribution of the D peak intensity is shown in Fig. 3(d) and indicates that there is no significant change after annealing.

Back gated FET devices were fabricated on CVD graphene, and mobilities were extracted<sup>19</sup> before and after annealing. The annealing was performed in a different chamber than the electrical measurement apparatus and the devices were, thus, briefly exposed to air prior to measurement in the vacuum probe station. Measurements of 18 devices were carried out at a vacuum pressure of  $1 \times 10^{-5}$  mbar after a 12–24 h pumpdown, with careful attention to potential systematic errors previously reported for mobility measurements.<sup>19</sup> A representative transfer curve is shown in Fig. 4(a).

The as-transferred CVD graphene exhibits a shift of the minimum conductivity (MC) point to positive voltage and is attributed to p-type doping from fixed charge in the residual PMMA that also results in an increase in carrier scattering, reducing the field effect mobility of graphene. Field effect mobilities were measured with a mean value of  $1413 \text{ cm}^2/\text{Vs}$  for these unannealed devices. Prior reports indicate that PMMA can be a source of p-type doping.<sup>20–22</sup> The interaction of oxygen, a PMMA constituent, as well as moisture with graphene has also been reported to result in p-type dopant effects.<sup>18</sup> Such species are anticipated to be effectively removed from the CVD graphene surface by suitable vacuum annealing.<sup>5,11,12</sup>

Upon annealing, electrical measurements under vacuum indicate that there is a reduction in p-type doping, while Raman measurements indicate an increase in p-type doping. This apparent discrepancy is attributed to two competing effects. First, the vacuum anneal process results in the desorption of PMMA residue from the surface as well as potentially trapped H<sub>2</sub>O and/or O<sub>2</sub> at the graphene/SiO<sub>2</sub> interface and, thus, leads to a reduction in p-type doping. Second,<sup>18</sup> the increase in sensitivity to hole doping by reversibly adsorbed species such as O<sub>2</sub> at this interface may lead to a

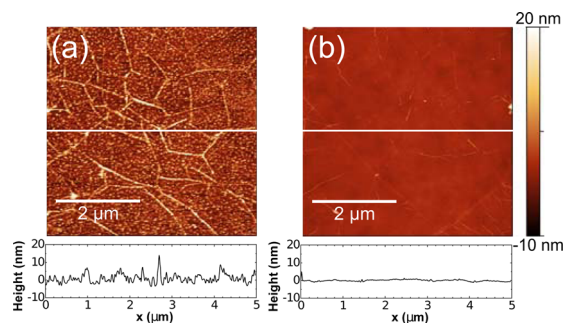


FIG. 2. (Color online) AFM images of (a) graphene after transfer to SiO<sub>2</sub> and acetone PMMA strip (RMS roughness=4.6 nm) and (b) as in (a) plus 300 °C/3 h UHV anneal (RMS=0.6 nm).

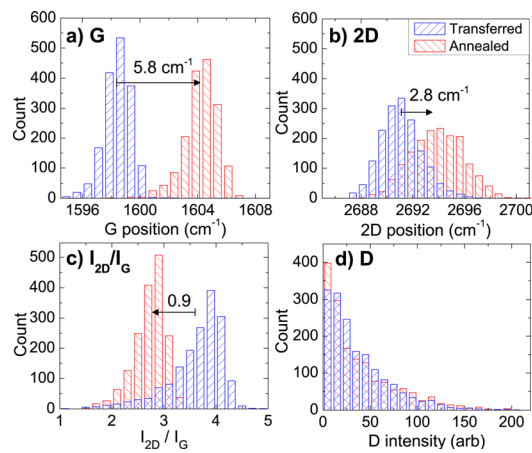


FIG. 3. (Color online) Histogram distributions extracted from Raman map data for (a) G and (b) 2D peak positions, (c)  $I_{2D}/I_G$  intensity ratio, and (d) D peak intensity before and after anneal at 300 °C for 3 h in UHV.

large increase in p-type doping for Raman measurements carried out in air. A reduction of hysteresis in the DC  $R_{Total}$ - $V_{GS}$  transfer curve (not shown) as well as increased symmetry about the MC point is also observed. Accordingly, the field effect mobility increased with a mean of 2714  $cm^2/Vs$  (Fig. 4(b)). Moreover, the post-anneal negative shift of the MC point voltage (Fig. 4(c)), the reduction of the carrier concentration (Fig. 4(d)), and the removal of electron-hole conduction asymmetry<sup>21</sup> strongly suggest that the PMMA residue is substantially responsible for the p-type doping observed in transferred CVD graphene devices.

In order to more clearly distinguish the role of PMMA from other sources of scattering sources such as water trapped at the graphene/SiO<sub>2</sub> interface, PMMA was re-spun on the annealed devices and then removed using acetone/IPA as described in the transfer process. After this step, the mobility dropped to a mean value of 2056  $cm^2/Vs$ , greater than the mean pre-anneal mobility but lower than the post-anneal mobility (Fig. 4). The electrical results after re-exposure to PMMA indicate that the residual PMMA clearly plays a significant role in p-type chemical doping of transferred CVD graphene, while trapped species at the graphene/SiO<sub>2</sub> interface are also important.

It is shown that vacuum annealing is an effective method for the reduction of PMMA residue from transferred CVD graphene. The removal of this residue leads to a 2 × increase in carrier mobility. While PMMA residue plays a significant role in the mobility of transferred graphene, scattering from other charged species, such as adsorbed O<sub>2</sub> and trapped H<sub>2</sub>O, must also be considered.

The authors acknowledge the discussions on corroborating IR data with Ms. M. Acik and Y. J. Chabal as well as access to the Raman spectrometer. Useful discussions with Mr. S. Jandhyala and Mr. G. Mordi are also acknowledged. This work is sponsored by the Nanoelectronic Research Initiative (NRI SWAN Center) and the Office of Naval Research. C. W. Magnuson is supported by the Laboratory Directed Research and Development program of Sandia National Laboratories.

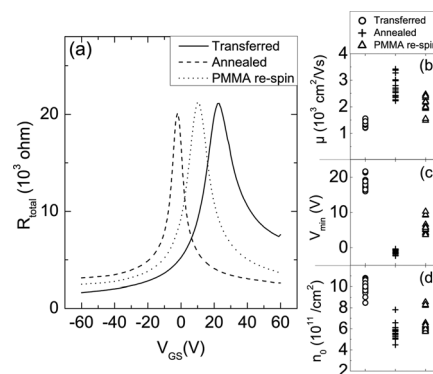


FIG. 4. (a) Back-gated graphene FET measurements under vacuum carried out for transferred CVD graphene (solid curve), after 300 °C/3 h UHV anneal (dashed curve) and after re-spinning PMMA and removing with acetone (dotted curve). Summary of extracted parameters for 17 devices showing (b) field effect mobility, (c) minimum conductivity point ( $V_{min}$ ), and (d) intrinsic carrier concentration.

- <sup>1</sup>X. Li, W. Cai, J. An, S. Kim, J. Nah, D. Yang, R. Piner, A. Velamakanni, I. Jung, E. Tutuc, S. K. Banerjee, L. Colombo, and R. S. Ruoff, *Science* **324**, 1312 (2009).
- <sup>2</sup>X. Li, C. W. Magnuson, A. Venugopal, J. An, J. W. Suk, B. Han, M. Borysiak, W. Cai, A. Velamakanni, Y. Zhu, L. Fu, E. M. Vogel, E. Voelkl, L. Colombo, and R. S. Ruoff, *Nano Lett.* **10**, 4328 (2010).
- <sup>3</sup>H. Cao, Q. Yu, L. A. Jauregui, J. Tian, W. Wu, Z. Liu, R. Jalilian, D. K. Benjamin, Z. Jiang, J. Bao, S. S. Pei, and Y. P. Chen, *Appl. Phys. Lett.* **96**, 122106 (2010).
- <sup>4</sup>H. Cao, Q. Yu, R. Colby, D. Pandey, C. S. Park, J. Lian, D. Zemlyanov, I. Childres, V. Drachev, E. A. Stach, M. Hussain, H. Li, S. S. Pei, and Y. P. Chen, *J. Appl. Phys.* **107**, 044310 (2010).
- <sup>5</sup>J. Kedzierski, P. L. Hsu, A. Reina, J. Kong, P. Healey, P. Wyatt, and C. Keast, *IEEE Electron Device Lett.* **30**, 745 (2009).
- <sup>6</sup>A. Avsar, T. Y. Yang, S. Bae, J. Balakrishnan, F. Volmer, M. Jaiswal, Z. Yi, S. R. Ali, G. Gulntherodt, B. H. Hong, B. Beschoten, and B. Olzylmaz, *Nano Lett.* **11**, 2363 (2011).
- <sup>7</sup>Y. G. Lee, C. G. Kang, U. J. Jung, J. J. Kim, H. J. Hwang, H.-J. Chung, S. Seo, R. Choi, and B. H. Lee, *Appl. Phys. Lett.* **98**, 183508 (2011).
- <sup>8</sup>S. Adam, E. Hwang, V. Galitski, and S. Das Sarma, *Proc. Natl. Acad. Sci. U.S.A.* **104**, 18392 (2007).
- <sup>9</sup>M. Lafkioti, B. Krauss, T. Lohmann, U. Zschieschang, H. Klauk, K. v. Klitzing, and J. H. Smet, *Nano Lett.* **10**, 1149 (2010).
- <sup>10</sup>J. W. Suk, A. Kitt, C. W. Magnuson, Y. Hao, S. Ahmed, J. H. An, A. Swan, B. Goldberg, and R. S. Ruoff, *ACS Nano* (2011).
- <sup>11</sup>Z. Cheng, Q. Zhou, C. Wang, Q. Li, C. Wang, and Y. Fang, *Nano Lett.* **11**, 767 (2011).
- <sup>12</sup>M. Ishigami, J. H. Chen, W. G. Cullen, M. S. Fuhrer, and E. D. Williams, *Nano Lett.* **7**, 1643 (2007).
- <sup>13</sup>A. Nourbakhsh, M. Cantoro, A. Klekachev, F. Clemente, B. Sorele, M. H. van der Veen, T. Vosch, A. Stesmans, B. Sels, and S. De Gendt, *J. Phys. Chem. C* **114**, 6894 (2010).
- <sup>14</sup>S. Doniach and M. Sunjic, *J. Phys. C* **3**, 285 (1970).
- <sup>15</sup>G. Beamson, A. Bunn, and D. Briggs, *Surf. Interface Anal.* **17**, 105 (1991).
- <sup>16</sup>T. Kashiwagi, A. Inaba, J. E. Brown, K. Hatada, T. Kitayama, and E. Masuda, *Macromolecules* **19**, 2160 (1986).
- <sup>17</sup>A. Das, S. Pisana, B. Chakraborty, S. Piscanec, S. Saha, U. Waghmare, K. Novoselov, H. Krishnamurthy, A. Geim, A. Ferrari, and A. K. Sood, *Nat. Nanotechnol.* **3**, 210 (2008).
- <sup>18</sup>S. Ryu, L. Liu, S. Berciaud, Y. J. Yu, H. Liu, P. Kim, G. W. Flynn, and L. E. Brus, *Nano Lett.* **10**, 4944 (2010).
- <sup>19</sup>A. Venugopal, J. Chan, X. Li, C. W. Magnuson, W. P. Kirk, L. Colombo, R. S. Ruoff, and E. M. Vogel, *J. Appl. Phys.* **109**, 104511 (2011).
- <sup>20</sup>M. Na and S. W. Rhee, *Org. Electron.* **7**, 205 (2006).
- <sup>21</sup>D. B. Farmer, R. Golizadeh-Mojarad, V. Perebeinos, Y.-M. Lin, G. S. Tulevski, J. C. Tsang, and P. Avouris, *Nano Lett.* **9**, 388 (2009).
- <sup>22</sup>J. Chen, M. Ishigami, C. Jang, D. R. Hines, M. S. Fuhrer, and E. D. Williams, *Adv. Mater.* **19**, 3623 (2007).